

Influence of nano-oxide layer on the giant magnetoresistance and exchange bias of NiMn/Co/Cu/Co spin valve sensors

Anoop Gupta,^{1,a)} Senthilnathan Mohanan,¹ Michael Kinyanjui,² Andrey Chuvilin,² Ute Kaiser,² and Ulrich Herr¹

¹*Institute of Micro and Nanomaterials, Ulm University, 89081 Ulm, Germany*

²*Electron Microscopy Group of Material Science, Ulm University, 89081 Ulm, Germany*

(Received 8 October 2009; accepted 25 March 2010; published online 6 May 2010)

NiMn is an interesting material for achieving a high exchange bias in spin valve systems. We investigated the influence of a nano-oxide layer (NOL) inserted in the pinned Co layer on the magnetotransport properties of NiMn/Co/Cu/Co spin valve sensors. The samples were annealed at 350 °C for 10 min to achieve the antiferromagnetic L1₀ ordered structure of NiMn. The NOL has been characterized by small angle x-ray reflectivity, transmission electron microscopy (TEM), and energy filtered TEM. The inclusion of the NOL leads to an increase in the giant magnetoresistance (GMR) by 20 % indicating a high degree of specular reflection at the NOL. For NOL positions close to the NiMn/Co interface, a decrease in the exchange bias field (H_{ex}) is observed. The best combination of high GMR value and large H_{ex} was found when the NOL was inserted in the center of the pinned Co layer. © 2010 American Institute of Physics. [doi:10.1063/1.3407569]

I. INTRODUCTION

Giant magnetoresistance (GMR) has evoked intense interest from researchers in fundamental physics as well as for industrial applications, such as read head sensors and the magnetic random access memory.¹ In the case of spin valve read head sensors, the operating temperature can reach high values due to heating by the sensing current and electrostatic discharge.² Therefore, they require a high thermal stability and a sufficient exchange bias field (H_{ex}) even at elevated temperature. In recent years, several antiferromagnetic (AFM) materials have been used as pinning layers.³⁻⁵ Among these, NiMn in the L1₀ ordered phase is a promising AFM material due to its large H_{ex} , high blocking temperature, excellent thermal stability, and good corrosion resistance.⁶ In NiMn films the disordered fcc phase is found which exhibits paramagnetic behavior. Therefore, the films have to be annealed at temperatures around 300 °C in order to obtain the equilibrium L1₀ ordered AFM phase. This may lead to interdiffusion across the interfaces which deteriorates the magnetic characteristics of the sensors.⁷ A possible solution to this problem is a combination of conventional annealing and irradiation with ultrashort laser pulses, which leads to improved magnetic properties.⁸ Another solution may be the insertion of a nano-oxide layer (NOL) into the pinned ferromagnetic layer. It has been reported that the NOL may act as a diffusion barrier which can prevent interdiffusion across the interfaces.⁹ In addition, the NOL enhances the magnetoresistance ratio due to specular electron scattering at the NOL/ferromagnet interface.¹⁰ In earlier studies the NOL has been introduced into spin valve structures with Fe based alloys, where the magnetic layers have been coupled ferromagnetically across the NOL through the Fe oxide.⁹⁻¹² In

this study, we incorporated the NOL into the pinned Co layer of NiMn/Co/Cu/Co GMR spin valve sensors by oxidation in pure O₂ at low pressures. We systematically studied the influence of the NOL on magnetotransport properties and exchange bias field by varying the O₂ exposure time and the position of the NOL in the pinned Co layer. Whereas in earlier work no GMR has been observed for IrMn/Co based bottom pinned spin valves with NOL in the Co layer,¹³ we find an enhanced GMR in our study.

II. EXPERIMENT

In this study, top spin valves with the layer structure of Ta(7.0 nm)/Co(5.1 nm)/Cu(2.1 nm)/Co(2.55 nm)/NOL/Co(2.55 nm)/NiMn(25 nm) were deposited on Si substrates by dc magnetron sputtering at room temperature. The base pressure was about 10⁻⁷ mbar and the Ar pressure during deposition was 10⁻³ mbar. The NOL was formed by exposing the Co layer to pure O₂ atmosphere in the load lock chamber with an O₂ flow rate of 5 SCCM (SCCM denotes cubic centimeter per minute at STP) and a pressure of 10⁻² mbar for varying O₂ exposure time from 20 s up to 300 s. To achieve L1₀ ordering of the NiMn, post deposition annealing was carried out at a temperature of 350 °C for 10 min in vacuum better than 5 × 10⁻⁶ mbar without external applied field; previous results⁸ showed that large exchange bias fields may be obtained under these conditions. The transport properties were measured using standard four probe technique in current in-plane geometry. The magnetic properties were determined using a vibrating sample magnetometer (LakeShore 735). Angular dependent hysteresis loops have been measured for all samples in the as-prepared state. For each sample, a square hysteresis loop with sharp switching field was observed in a certain direction, which is characteristic for the existence of an easy axis. The easy axis may originate from the magnetic field experienced during magnetron sputtering, the stress induced in the Co layer during

^{a)} Author to whom correspondence should be addressed. Tel.: +49 203 379 3769. FAX: + 49 203 379 3087. Electronic mail: anoop.gupta@uni-due.de.

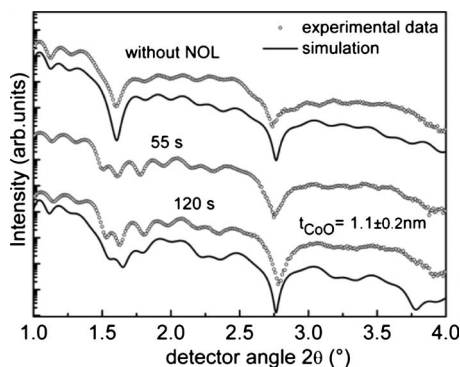


FIG. 1. SAXR spectra (open circles) and simulations (solid lines) of as-prepared sample without NOL and with NOL formed after O_2 exposure during duration of 55 and 120 s.

deposition or the columnar growth of the Co film.^{14–16} The GMR measurements were carried out at room temperature with the field applied parallel to the easy axis. Small angle x-ray reflectivity (SAXR) measurements were performed using a Siemens D5005 diffractometer with $Cu K_\alpha$ radiation. Cross sectional transmission electron microscopy (TEM) images have been obtained using a Philips CM20 operated at an accelerating voltage of 200 kV. The concentration profile analysis has been carried out by energy filtered TEM (EFTEM) in a Titan 80–300 operated at an accelerating voltage of 300 kV.

III. RESULTS AND DISCUSSION

Figure 1 shows SAXR curves for an as-prepared sample without NOL and two samples with NOL, which were formed after an O_2 exposure time of 55 and 120 s. There was a significant difference between the SAXR spectra with and without NOL, whereas no observable changes were found with increasing O_2 exposure time. This indicates that there was no significant change in the thickness of the NOL with increasing oxidation time. The simulated intensities shown in Fig. 1 have been calculated using the REFSIM software based on the Parrat algorithm. A good match is found between simulated curves and experimental results with the individual layer thicknesses from the preparation process. The thickness of the NOL obtained from the simulation is 1.1 ± 0.2 nm.

Figure 2 shows the cross sectional TEM image of the as-prepared sample with NOL obtained after 120 s of O_2

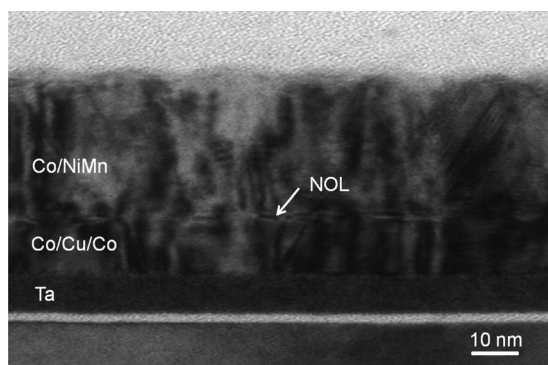


FIG. 2. Cross-sectional TEM image of as-prepared sample with NOL obtained after O_2 exposure for 120 s.

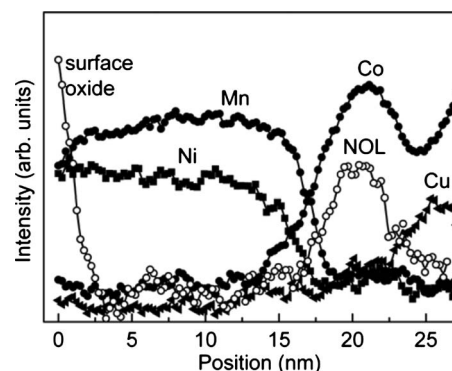


FIG. 3. Concentration profile for Co, Cu, Ni, Mn, and O of the annealed sample with NOL (obtained after O_2 exposure for 120 s) in the middle of pinned Co layer.

exposure time. The NOL can be identified as a narrow and discontinuous white stripe in the image. The thickness of the NOL was about 1–1.5 nm, which corresponds well with the value obtained from the SAXR spectra. It is also observed from Fig. 2 that the columnar growth of the multilayer was not significantly interrupted by the insertion of the NOL.

In order to obtain the AFM $L1_0$ ordered phase of the NiMn, all samples were annealed at $350^\circ C$ for 10 min. Figure 3 shows the concentration profiles for a sample with NOL obtained by 120 s of O_2 exposure after the annealing treatment, which have been determined from EFTEM. Concentration profiles of the individual elements have been derived from the element specific images. The concentrations of Co, Cu, Ni, Mn, and O are shown as a function of the distance from the top of the sample. We observed a sharp decrease in the concentrations of Mn and Ni at the transition to the Co layer and the NOL. We note that due to the limited resolution of the EFTEM measurement there is some overlap between the signals of the NiMn layer, the first part of the Co layer (which is only 2.55 nm thick) and the NOL. However, it can be observed in Fig. 3 that the Mn signal extends to larger position values (i.e., depth from the top of the spin valve structure) than the Ni signal. Jang *et al.*⁹ and Dai *et al.*¹¹ reported that Mn diffuses upon annealing and forms manganese oxide within the NOL. Mn diffusion in IrMn/CoFe/Cu/CoFe type spin valves has been studied in detail by three-dimensional atom probe by You *et al.*¹⁷ Diffusion of Mn over large distances (9 nm) was found after annealing at $245^\circ C$ for 5 h. You *et al.* suggest that the preferential oxidation of Mn due to its strong affinity to oxygen was the reason for the enhanced diffusivity of Mn.

In order to study the effect of annealing on the NOL in our samples in detail, we have investigated a sample oxidized for 120 s before and after annealing by SAXR. Figure 4 shows the SAXR spectra and corresponding simulations in the as-prepared and the annealed state of the NiMn/Co/Cu/Co sample. The results of the fits to the SAXR data showed an increase in the roughness of the individual layers of about 0.3 nm during the annealing. No significant change in the layer thicknesses was found. This indicates that the NOL does not change its thickness or position significantly during the annealing treatment. It is well known that an increase in interface roughness or interdiffusion across the in-

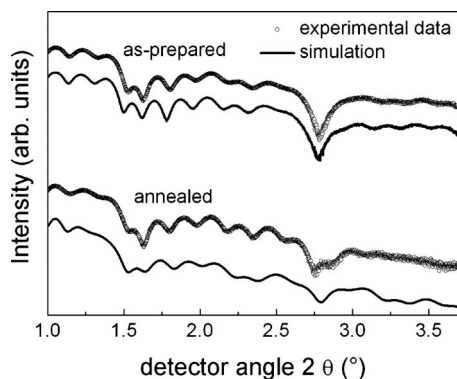


FIG. 4. SAXR spectra (open circles) and simulations (solid lines) in as-prepared and annealed state of NiMn/Co/Cu/Co sample with NOL formed by oxidation for 120 s.

interfaces may lead to very similar effects in (specular) SAXR measurements. In particular, they can both cause a reduction in the intensity of the interference maxima. The increase in the layer roughness found from the fits to the SAXR measurements may therefore also be a result of some interdiffusion of the individual elements in the spin valve structure.

Figure 5 shows a comparison of the GMR curves for samples with and without NOL after annealing. It is observed that the GMR increases for the sample with the NOL but the width of the plateau region decreases. In addition, the center position of the pinned layer hysteresis loop shifts to lower fields, indicating a reduction in the exchange bias field H_{ex} . The sharp switching behavior of the pinned Co layer in the sample with NOL indicates the existence of strong ferromagnetic coupling between the two parts of the pinned Co layer across the NOL, possibly through pinholes in the NOL.¹⁸

Figure 6 shows the values of GMR and H_{ex} as a function of O_2 exposure time. Figure 6(a) shows that the GMR increases from 7.5% to 9% with increasing O_2 exposure time up to 35 s, beyond which there was no significant change. This corresponds to a relative increase in the GMR by 20% after insertion of the NOL into the pinned Co layer. The increase in the GMR can be attributed to the specular electron scattering at the Co/NOL interface. The relative increase in 20% and the absolute GMR values compare well with the results of Wang *et al.*¹⁹ obtained for IrMn/CoFe/Cu/CoFe

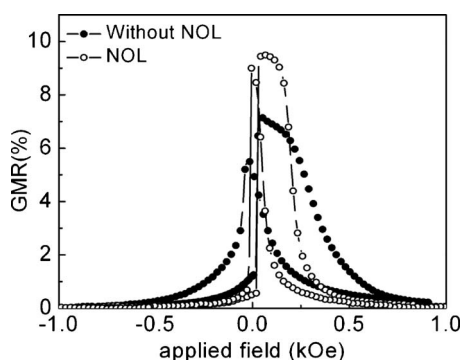


FIG. 5. GMR curves of annealed sample with NOL (open symbols) and without NOL (filled symbols); arrows indicate the directions of the field sweep.

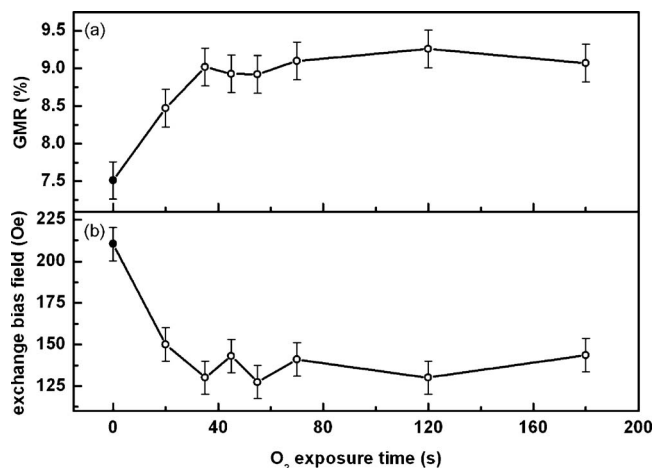


FIG. 6. (a) GMR and (b) H_{ex} as a function of oxygen exposure time. The filled symbols represent the values of the sample without NOL.

spin valves. Wang *et al.* find a maximum increase in the GMR from 6% to about 9% by inclusion of the NOL in the pinned CoFe layer. Their calculations show that the result is consistent with an increase in the electron mean free path by specular reflection at the NOL. According to these calculations, an increase in the GMR of 20% requires a (specular) reflectivity of the NOL of around 50% (assuming spin-independent scattering at the NOL). Figure 6(b) shows that H_{ex} decreases from 210 Oe to a constant value of about 140 Oe with increasing O_2 exposure time. The constant values of GMR and H_{ex} after 35 s of O_2 exposure correspond well with the constant thickness of the NOL as observed in the SAXR measurement. We also observed that after O_2 exposure for 240 s or more, the value of H_{ex} drops to values of about 60 Oe (not shown in Fig. 6), whereas the GMR value remains constant. We attribute the additional drop of H_{ex} for exposure time of 240 s and more to an increased O_2 uptake.

In order to study the influence of the position of the NOL, samples with the structure Ta(7.0 nm)/Co(5.1 nm)/Cu(2.1 nm)/Co_{P1}(5.5 - x nm)/NOL/Co_{P2}(x nm)/NiMn(25 nm) were prepared. In this series of samples, the total thickness of the pinned layer was kept constant, and only the position of the NOL has been varied. Oxygen exposure time was kept constant at 120 s for all the samples, and the samples have been subsequently annealed at 350 °C for 10 min. Figure 7(a) shows that the GMR increases as the NOL position approaches the Co/NiMn interface. This result compares well with the findings of Wang *et al.*¹⁹ on CoFe/Cu/CoFe spin valves and Suh and Ross²⁰ on NiFe/Cu/Co (pseudo) spin valves. Wang *et al.* have also observed that the GMR vanishes when the NOL approaches the interface between the pinned FM layer and the Cu spacer layer. In our work, we observe a similar trend as the GMR falls below the value without NOL insertion [7.5%, see Fig. 7(a)] when the NOL was positioned at about 1 nm distance from the Cu/Co interface. We note that Gillies and Kuiper¹³ reported earlier that they did not observe GMR in IrMn based bottom pinned spin valves with NOL in a pure Co layer. Comparing the work of Gillies *et al.* with our work, we find that there are some differences in the preparation conditions. Most importantly, the annealing treatments differ

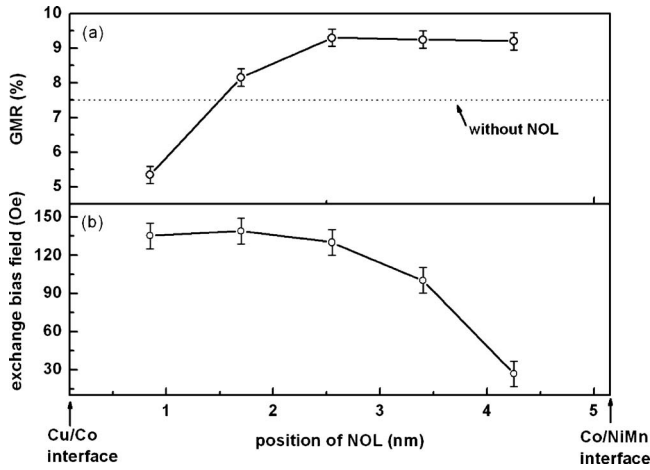


FIG. 7. (a) GMR and (b) H_{ex} as a function of the position of the NOL. The horizontal line in Fig. 7(a) represents the GMR without NOL insertion.

between both works: Gillies and Kuiper annealed their samples at 300 °C for 5 s, whereas our annealing treatment was done at 350 °C for 10 min. This may lead to different amounts of interdiffusion of the constituents in both cases. Also, it appears that Gillies *et al.* oxidized their pure Co samples in air, whereas our samples were oxidized in dry oxygen at low pressure. We believe that the differences between the conditions used in our study and Gillies and Kuiper's work make it difficult to conclude that our results contradict Gillies and Kuiper's earlier result. Further studies would be necessary to come to a final conclusion about the differences between both results.

Figure 7(b) shows the values of H_{ex} as a function of the NOL position. It is observed that H_{ex} decreases progressively as the NOL approaches the Co/NiMn interface. The optimum position for the NOL was found to be in the middle of the pinned Co layer; for this NOL position, we observed a high GMR value in combination with a sufficiently large H_{ex} .

For the discussion of the observed decrease in the H_{ex} , we refer to the well-known equation,²¹

$$H_{ex} = \frac{J_{ex} A_{Co-NiMn}}{M_s t_{Co} A_{Co}}, \quad (1)$$

where, J_{ex} is the exchange coupling constant, M_s is the saturation magnetization of Co, t_{Co} is the thickness of the pinned Co layer, A_{Co} is the cross sectional area of the pinned Co layer, and $A_{Co-NiMn}$ is the interfacial contact area between the NiMn and the pinned Co layer. One might expect that the NOL in the Co layer reduces the effective magnetic volume ($t_{Co} \times A_{Co}$) of the pinned Co layer by forming nonmagnetic Co oxide, which would lead to an increase in H_{ex} according to Eq. (1). However, our magnetization measurements did not show a significant difference in the M_s of Co between the sample with NOL and without NOL. Also, we observe a decrease in the H_{ex} for the sample with the NOL instead of an increase. The decrease in H_{ex} can only be caused by a decrease in J_{ex} or $A_{Co-NiMn}$ in Eq. (1).

A change in the stoichiometry of the NiMn at the Co/NiMn interface due to interdiffusion during the annealing treatment would change the degree of $L1_0$ ordering of the NiMn and hence the J_{ex} . Differences in the microstructure of

the NiMn layer after annealing (grain size or ordered domain size) might also affect the value of J_{ex} . In a previous study,²² we did a detailed structure characterization of annealed NiMn/Co/Cu/Co spin valve structures without NOL with emphasis on the ordering of the NiMn. We found that the size of ordered face centered tetragonal domains was significantly smaller than the size of the NiMn crystals. We do not expect that the grain size will change much by the incorporation of the NOL. This expectation is supported by the similarity of the increase in the surface roughness of the top pinned spin valve structures with or without NOL during annealing, as determined from the SAXR measurements; additional grain growth in the NiMn top layer would most likely also increase the surface roughness.

Alternatively, the decrease in H_{ex} for the samples with NOL can also be due to a reduction in the interfacial contact area $A_{Co-NiMn}$. Oxygen diffusion toward the Co/NiMn interface can lead to preferential oxidation of the Mn and formation of Mn oxide. This would also be in accord with the enrichment of Mn at the interface between NiMn layer and Co layer observed in the EFTEM (Fig. 3). We have made a similar observation in a recent study (unpublished) of NiMn surfaces annealed under high vacuum conditions ($p = 10^{-5}$ mbar), where we found formation of Mn oxide surface layers after annealing. This would decrease the number of pinning sites across NiMn/Co interface, which in turn would lead to a lower value of H_{ex} . The formation of a Mn oxide layer could also account for the dependence of H_{ex} on the NOL position inside the Co layer. Since the formation of the Mn oxide is a diffusion controlled process, the amount of Mn oxide formed during the annealing treatment depends on the distance between the NOL and the NiMn layer. This mechanism can also account for the observed decrease in H_{ex} for long exposure to O_2 (240 s and more) which may be a consequence of an increased amount of Mn oxide at the Co/NiMn interface under these conditions. Therefore, we conclude that the reduction in the H_{ex} observed under the annealing conditions used in this study is most likely a consequence of the diffusion of oxygen to the Co/NiMn interface.

IV. CONCLUSION

A NOL was successfully incorporated into the pinned Co layer of NiMn/Co/Cu/Co spin valves. We found that the GMR ratio can be significantly increased by incorporation of the NOL, which contrasts with earlier reports of IrMn/Co bottom pinned spin valves systems.¹³ The position of the NOL in the pinned Co layer significantly influences the GMR, which agrees well the results from earlier work on IrMn based spin valves. A maximum increase in the GMR value from 7.5 % to 9 % (corresponding to 20 % relative increase) has been found for insertion of the NOL in the center of the pinned Co layer. The insertion of the NOL leads to a decrease in the exchange bias field H_{ex} . The decrease in H_{ex} depends on the distance between the NOL and the Co/NiMn interface, which can be explained by the effect of oxygen diffusion toward the Co/NiMn interface during the

annealing treatment. The best combination of large GMR and H_{ex} values is observed when the NOL was inserted in the center of the pinned Co layer.

ACKNOWLEDGMENTS

The authors gratefully acknowledge financial support by the Landesstiftung Baden-Württemberg, Germany.

- ¹J. C. S. Kools, *IEEE Trans. Magn.* **32**, 3165 (1996).
- ²R. W. Cross, Y. K. Kim, J. O. Oti, and S. E. Russek, *Appl. Phys. Lett.* **69**, 3935 (1996).
- ³S. Araki and M. Sano, *IEEE Trans. Magn.* **34**, 1426 (1998).
- ⁴H. Kishi, Y. Kitade, Y. Miyake, A. Tanaka, and K. Kobayashi, *IEEE Trans. Magn.* **32**, 3380 (1996).
- ⁵C. H. Lin, P. C. Kuo, and J. S. Huang, *IEEE Trans. Magn.* **31**, 2916 (1995).
- ⁶A. J. Devasahayam and M. H. Kryder, *IEEE Trans. Magn.* **35**, 649 (1999).
- ⁷C. Loch, W. Maass, B. Ocker, and K. Röhl, *J. Appl. Phys.* **85**, 4460 (1999).
- ⁸S. Mohanan, R. Diebold, R. Hibst, and U. Herr, *J. Appl. Phys.* **103**, 07B502 (2008).
- ⁹S. H. Jang, T. Kang, H. J. Kim, and K. Y. Kim, *Appl. Phys. Lett.* **81**, 105 (2002).
- ¹⁰A. Veloso, P. P. Freitas, P. Wei, N. P. Barradas, J. C. Soares, B. Almeida, and J. B. Sousa, *Appl. Phys. Lett.* **77**, 1020 (2000).
- ¹¹B. Dai, J. W. Cai, W. Y. Lai, F. Shen, Z. Zhang, and G. H. Yu, *Appl. Phys. Lett.* **82**, 3722 (2003).
- ¹²D. H. Lee, S. Y. Yoon, J. H. Kim, and S. J. Suh, *Thin Solid Films* **475**, 251 (2005).
- ¹³M. F. Gillies and A. E. T. Kuiper, *J. Appl. Phys.* **88**, 5894 (2000).
- ¹⁴C.-H. Lai, S.-A. Chen, and J. C. A. Huang, *J. Magn. Magn. Mater.* **209**, 122 (2000).
- ¹⁵M. Takahashi, *J. Appl. Phys.* **33**, 1101 (1962).
- ¹⁶S. Jo, Y. Choi, and S. Ryu, *IEEE Trans. Magn.* **33**, 3634 (1997).
- ¹⁷C. Y. You, A. Cerezo, P. H. Clifton, L. Folks, M. J. Carey, and A. K. Petford-Long, *Appl. Phys. Lett.* **91**, 011905 (2007).
- ¹⁸J. C. S. Kools, S. B. Sant, K. Rook, W. Xiong, F. Dahmani, W. Ye, J. Nunez-Regueiro, Y. Kawana, M. Mao, K. Koi, H. Iwasaki, and M. Sashiki, *IEEE Trans. Magn.* **37**, 1783 (2001).
- ¹⁹L. Wang, J. J. Qiu, W. J. McMahon, K. B. Li, and Y. H. Wu, *Phys. Rev. B* **69**, 214402 (2004).
- ²⁰J. D. Suh and C. A. Ross, *Phys. Status Solidi* **244**, 4474 (2007) (b).
- ²¹A. E. Berkowitz and K. Takano, *J. Magn. Magn. Mater.* **200**, 552 (1999).
- ²²A. Gupta, A. Chuvilin, S. Mohanan, Z. Zhang, U. Kaiser, and U. Herr, *Sci. Adv. Mater.* **1**, 198 (2009).